ELSEVIER

European Journal of Pharmacology 328 (1997) 163–174

ejp

Long-term therapy with trimetazidine in cardiomyopathic Syrian hamster BIO 14:6

Nathalie D'hahan [a,b,*], Karima Taouil [a,b], Abdelilah Dassouli [a,b], Jean-Emile Morel [a,b]

[a] *Laboratoire de Biologie, Ecole Centrale de Paris, 92295 Châtenay-Malabry, France*

[b] *Département de Biologie Cellulaire et Moléculaire, Service de Biophysique des Protéines et des Membranes, CE-Saclay, 91191 Gif-sur-Yvette Cedex, France*

Received 22 January 1997; revised 25 March 1997; accepted 28 March 1997

Abstract

The cardiomyopathic Syrian hamster (CMH) of the strain BIO 14:6 is a model for both cardiac and skeletal muscle abnormalities. It has reduced longevity and noticeable hypertrophy of the heart and liver. At 220 days, CMHs display a total Ca^{2+} overload, 1.3–1.8-fold normal and a cytosolic Ca^{2+} concentration 2–4-fold higher than normal. Long-term oral treatment (18 mg/kg per day) with trimetazidine (anti-ischaemic drug), from age 30 to 350 days, was more efficient than the standard Ca^{2+} blocker verapamil. Trimetazidine increased the median survival time of CMH by 57% and the hypertrophy disappeared. The total Ca^{2+} level in CMHs reverted to that of normal Syrian hamsters (F1B). The cytosolic Ca^{2+} overload was limited to a factor of $\cong 2$. Therefore, trimetazidine possesses anti-Ca^{2+} properties and is effective in increasing survival and decreasing the heart and liver hypertrophy of CMH. This suggests that trimetazidine may be valuable in the prevention of congestive heart failure of similar aetiology. © 1997 Elsevier Science B.V.

Keywords: Cardiomyopathy; Ca^{2+}; Hypertrophy; Ischemia; Trimetazidine; Verapamil

1. Introduction

Many authors have described hypertrophic cardiomyopathy as a chronic ischaemic disorder (Natelson et al., 1991; Conway et al., 1994). Drug therapy for this disease has improved over the last 20 years. β-Adrenoceptor antagonists, Ca^{2+} channel antagonists (Sonnenblick et al., 1985) and long-acting nitrates (Hanton et al., 1993) act mainly through a haemodynamic mechanism (coronary dilatation, reduced peripheral resistance) that induces a reduction of myocardial oxygen consumption during effort. They also have cardiodepressant activity and/or may aggravate coronary artery spasms or may cause lowering of blood pressure, headache, tachycardia and peripheral oedema in some patients (Van Zwieten, 1985; Boddeke et al., 1989). Therefore, there have been numerous experimental investigations to identify drugs with similar antianginal properties, but without such drawbacks (Chiercha and Fragasso, 1993). Trimetazidine, 1-(2,3,4-trimethoxybenzyl) piperazine di-hydrochloride, used in clinical treatment of anginal disease (Dalla-Volta et al., 1990; Detry et al., 1994), improves the clinical status of patients with severe ischaemic cardiomyopathy (Brottier et al., 1990), although the mechanisms underlying the positive effects of trimetazidine remain unknown (Fantini et al., 1994). Trimetazidine improves performance capacity in angina pectoris, as demonstrated by a significant increase in the duration of exercise, the total work performance and the improvement in electrocardiogram signs of ischaemia. In sharp contrast with other commonly used antianginal drugs, trimetazidine neither reduces oxygen consumption nor increases blood supply: no significant changes in heart rate, blood pressure or rate-pressure product have been observed at rest or during exercise (Detry et al., 1994). The effects may be due to protection of myocardial cell function during ischaemia by prevention of the fall in the ATP concentration (Lavanchy et al., 1987), limitation of the free radical concentration (Maupoil et al., 1990; Devynck et al., 1993) and prevention of the accumulation of Na^{+} and Ca^{2+} in the myocyte (Renaud, 1988). The goal of this study was to determine the effects in cardiomyopathic Syrian hamsters of long-term oral therapy with trimetazidine on survival, hypertrophy and abnormal intracellular Ca^{2+} levels. Trimetazidine was compared to verapamil, a well-known Ca^{2+} channel antagonist that is also used as

* Corresponding author at address a. Tel.: (33-1) 4113-1151; Fax: (33-1) 4113-1437.

an anti-anginal agent. BIO 14:6 cardiomyopathic hamsters (CMH), a widely used animal model for hypertrophic cardiomyopathy (Kagiya et al., 1991; Davidoff and Gwathmey, 1994), were used and compared to healthy golden hamsters (F1B), both treated for 220 and 350 days.

2. Materials and methods

2.1. Animals

Experiments were performed on male cardiomyopathic hamsters of the BIO 14:6 strain (CMH), purchased in Olivet (France); healthy Syrian golden hamsters (F1B) (Depré, France) were used as controls. All animals were individually housed at CE-Saclay under identical controlled conditions and on standard laboratory diet. They were then transferred to the Biology Laboratory of the Ecole Centrale de Paris, where they were killed and investigated. Thus, we could not study animals immediately after death.

2.2. Study design

The experimental design is presented in Fig. 1. The longest treatment was 350 days and the dose was increased during the study in all groups (see Section 2.3.1).

2.2.1. Experiment 1

The survival rate was studied using 33 CMH, 20 trimetazidine-treated CMH, 10 verapamil-treated CMH and 10 CMH treated with the combination trimetazidine + verapamil. Animals were weighed weekly until death. Healthy hamsters live about 2–3 years.

2.2.2. Experiment 2

The development of hypertrophy in CMH and normal F1B hamster controls was monitored in five pathological stages (cited in Venkatakrishnan and Rourke, 1979). Body, heart, liver and lung weights were determined after 30 days, the prenecrotic stage (3 CMH and 3 F1B), 65 days, the necrotic stage (3 CMH and 3 F1B), 140 days, the hypertrophic stage (5 CMH and 5 F1B), 220 days (17 CMH and 14 F1B) and 350 days (23 CMH and 8 F1B), the final stage. The effects of trimetazidine and verapamil were analysed using F1B and CMH at 220 days and 350 days, the time points where CMH exhibit well-established cardiac disease.

Protocol a: Five CMH and 4 F1B received trimetazidine (18 mg/kg per day) administered in the drinking water from age of 30 days to 220 days. Nine CMH and 4 F1B similarly received verapamil (120 mg/kg per day) and 7 CMH and 4 F1B, trimetazidine + verapamil (same doses).

Protocol b: Five CMH and 4 F1B received trimetazidine (18 mg/kg per day) administered in the drinking water from age of 30 days to 350 days. Four CMH and 4 F1B similarly received verapamil (120 mg/kg per day) and 4 CMH and 4 F1B, trimetazidine + verapamil (same doses).

Experiment 3. The intracellular Ca^{2+} analysis was performed on 220-day-old CMH and F1B animals, and on CMH treated from 30 to 220 days. Total Ca^{2+} content was measured in 12 F1B, 16 CMH, 8 trimetazidine-treated

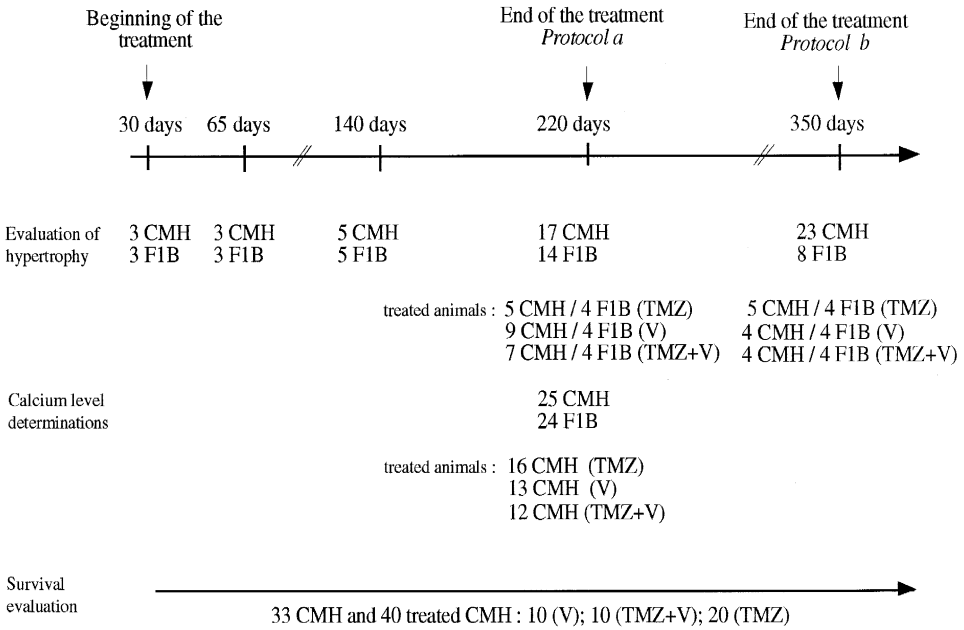

Fig. 1. Experimental design. The horizontal axis represents a time scale spanning the duration of the study. The type of experiment, the groups and the different time points studied are indicated.

CMH, 8 verapamil-treated CMH and 8 trimetazidine + verapamil-treated CMH. The cytosolic Ca^{2+} concentration was determined by spectrofluorometry for 8 F1B, 5 CMH, 8 trimetazidine-treated CMH, 5 verapamil-treated CMH and 4 trimetazidine + verapamil-treated CMH. Four F1B and 4 CMH were used to study intracellular Ca^{2+} levels by laser scanning cytometry.

2.3. Experimental protocol

2.3.1. Rationale for the trimetazidine and verapamil doses used

The dose of trimetazidine used for humans is 60 mg/24 h (3×20 mg), but no study of higher doses of trimetazidine has been conducted (IRIS, Institut de Recherches Internationales Servier, France). For the treatment of cardiomyopathy verapamil is used at doses between 240 and 360 mg/24 h. Linear animal to human conversion, based on body weight, has been shown to be inaccurate, unless complex conversion factors are applied. Nevertheless, rough approximations or predictions using a simple model with direct body weight comparisons can be obtained but should be used with caution when predicting human toxicity (Voisin et al., 1990). Moreover, doses should depend on the mode of administration. We administered the drugs in drinking water to minimize irritation and stress. We chose the verapamil dose on the basis of studies of oral therapy (Factor et al., 1988). A dose of 80 mg/kg was studied (1 g verapamil in 1 l of drinking water; average intake was 12 ml per day; average animal weight: 150 g), begun at 30 days to 220 days and 350 days. This dose did not prolong the survival of treated CMH beyond that of untreated CMH; doses increased by 50% from 80 days to 220 days were also tested (1.5 g in 1 l, i.e., 120 mg/kg) and were subsequently used in the study. For untreated CMH, extensive myocardial damage occurs between 70 and 150 days of age (Factor et al., 1988), and the 80 days time point was arbitrarily chosen. We administered verapamil throughout the period of active disease, as it is more protective than a therapy stopped at 100 or 150 days of age (Factor et al., 1988). The trimetazidine dose was calculated from the ratio between standard verapamil doses and standard trimetazidine doses administered to humans. The dose of trimetazidine was thus 12 mg/kg (0.12 g trimetazidine in 1 l of drinking water; average intake was 15 ml per day; average animal weight: 150 g). With this treatment, survival was not as satisfactory as expected in preliminary experiments and the dose was therefore increased by 50% after 80 days (0.18 g trimetazidine in 1 l, i.e., 18 mg/kg).

2.3.2. Serum trimetazidine and verapamil levels determination

Serum drug levels in CMH were determined. Three groups of 3 CMH (180–220 days old) were studied to determine trimetazidine concentrations in plasma after 8 days of treatment (group 1), after 18 days of treatment (group 2) and after 32 days of treatment (group 3), with 18 mg/kg per day. The plasma concentration of verapamil was determined in 220-day-old cardiomyopathic hamsters treated for 30 days with 120 mg/kg per day. Quantitative determination of trimetazidine and verapamil was done by gas chromatography and chemical ionization. The detection limit is 1 ng/ml in human blood, plasma or urine (Harpey et al., 1989).

2.4. Determination of hypertrophic state

Animals were anaesthetized with ether, their hearts (including both ventricles) were removed and, after the atria were dissected, weighed. Lungs and livers were also removed and weighed. Hypertrophy was determined by comparing the 'organ weight/body weight' ratios of CMH and F1B.

2.5. Cardiac myocyte isolation

220-day-old BIO 14:6 CMH ($n = 5$) and F1B ($n = 8$) were used for the determination of cytosolic Ca^{2+} concentration. Cardiac myocytes were isolated according to Sen et al. (1990). Normal and BIO 14:6 hamsters were anaesthetized with urethane (0.4 g/ml) and the hearts were rapidly removed. Isolated hearts were subjected to Langendorff retrograde arterial perfusion as follows: after cannulation of the aorta, hearts were perfused with oxygenated (95% O_2-5% CO_2), warm (37°C) low-Ca^{2+} Krebs-Henseleit bicarbonate-buffered solution (pH 7.3) containing (mM): NaCl (118); KCl (4.7); $CaCl_2$ (0.6); $MgSO_4$ (1.2); KH_2PO_4 (1.2); $NaHCO_3$ (25) and glucose (12). Note that the total calcium content (0.6 mM) corresponds partly to free Ca^{2+} and partly to calcium bound to anions, especially phosphate anion. About 10 min of perfusion (4 ml/min) was necessary to clear blood from the heart. Perfusion was continued for 40 min with the same buffer solution, except that the perfusate was changed to nominally zero-Ca^{2+} and 0.023% collagenase was added and recirculated through the heart. During this time the heart became swollen and pale. The ventricles were removed, cut into small pieces and placed in a flask containing 0.01% collagenase and 20 μM $CaCl_2$ in Krebs-Henseleit solution. The tissue fragments were shaken in a water bath at 37°C for 15 min. Tissue pieces were then placed in a Ca^{2+}-free buffer containing 0.05% collagenase and cells were disaggregated by gentle mechanical shaking. Warm (37°C) oxygenated Ca^{2+}-free buffer was added and the cells were centrifuged at 400 rpm for 1 min and the supernatant containing collagenase was removed. This washing was repeated twice. Cells (about 5×10^6 per heart) were then suspended in Ca^{2+}-free physiological Krebs buffer, containing 0.1% bovine serum albumin to improve viability. After 15 min, at least 80% of normal and cardiomyopathic cells were rod shaped. Viability was verified by the trypan blue (0.4% w/v) exclusion test. The

cell pellet was then suspended in a physiological buffer of the selected Ca^{2+} concentration (i.e., 0.6 mM). Cells were used on the day of isolation.

2.6. Intracellular Ca^{2+} analysis

2.6.1. Determination of cytosolic Ca^{2+} level

2.6.1.1. Measurement in a population of cells in suspension. The cytosolic Ca^{2+} concentration in cardiac myocytes was measured using the Ca^{2+}-sensitive fluorescent dye fura 2, which is a fluorescent tetracarboxylate chelator that exhibits a spectral shift in excitation maximum on Ca^{2+} binding. Measurements were done using disaggregated cells in suspension. Fura 2 was loaded into intact cells by incubation for 20 min at room temperature with the membrane-permeant ester derivative fura 2-AM (acetoxymethyl, AM) (2 μM) in a Krebs-buffer containing 0.1 mM $CaCl_2$ and 0.1% bovine serum albumin (according to Pocock and Nicholls, 1992). The cells were then washed twice in Krebs-buffered medium containing 0.6 mM $CaCl_2$, to remove extracellular dye, and transferred to a thermostated (20°C), stirred cuvette in a Hitachi Spectrofluorometer F-2000, with excitation wavelengths of 340 and 380 nm and an emission wavelength of 510 nm. The two excitation wavelengths were alternated once every second. The 340 nm/380 nm fluorescent intensity ratio was then converted into Ca^{2+} values by using the equation given by Grynkiewicz et al. (1985). To determine the relationship between the fura 2 ratio and the Ca^{2+} concentration, we titrated the dye released in vivo for calibration. The sequence of events was the following: (i) cells were placed in a zero-Ca^{2+} physiological buffer (containing 75 μM EGTA) and the ratio 340 nm/380 nm was measured (R); (ii) rapidly, to avoid large Ca^{2+} leakage, the detergent Triton X-100 (0.1%) and Ca^{2+} were added in excess to obtain the maximum fluorescence signal ratio (R_{max}); (iii) EGTA (20 mM) was added to obtain the minimum fluorescence signal ratio (R_{min}). At the end of each experiment, background autofluorescence from lysed cells was determined by addition of $MnCl_2$ (10 mM), which quenches the fluorescence of free fura 2, and the value obtained was subtracted from the raw signal values.

2.6.1.2. Measurement at the single cell level. Single cell analysis of Ca^{2+} was performed at Institut Pasteur, Paris, by interactive argon laser-based image analysis with a Meridian Instruments ACAS 570 cytometer, using cells identified with an inverted microscope and a ×100 objective. The aims were to visualize cytosolic Ca^{2+} levels in normal and cardiomyopathic cells (qualitative data) and to obtain comparative morphological and morphometric information on adherent control and cardiomyopathic cells. Cardiac cells were isolated from F1B ($n = 4$) and CMH ($n = 4$) as described for cell suspensions and placed in eight-well Lab-Tek coverglass chamber slides (Gibco, Cergy-Pontoise, France). Slides were first coated with laminin (20 μg/ml) supplemented with 10% foetal bovine serum and incubated for 45 min at room temperature. The diluted laminin-Krebs solution was then aspirated and the cell suspension in culture medium was added and kept at 37°C for 2–3 h. Attachment of the cells was checked under a microscope. Attached cells were then incubated in a Krebs buffer (300 μl/well) containing 2 μM indo 1-AM (acetoxymethyl, AM), for 20 min at room temperature. The cells were rinsed twice to remove excess indo 1-AM and placed in a final volume of 300 μl/well Krebs buffer containing 0.6 mM $CaCl_2$. Cytosolic Ca^{2+} was determined in each cell of interest, by exciting indo 1 at 361–364 nm and simultaneously detecting emission at 405 and 450 nm. The ratio of these emissions was computed by Meridian Ca^{2+} analysis Software. Morphological and morphometric information about adherent cells was recorded for normal and cardiomyopathic myocytes (Métézeau et al., 1993).

2.6.1.3. Methodological limitations. Some of the problems associated with the measurement of intracellular Ca^{2+} concentrations were overcome: a ratiometric fluorescence method and rapidly loading of cells at room temperature almost entirely reduced the effects of dye leakage, variable dye concentration, cell thickness and intracellular compartmentalization. The calculated values could be used for a comparative study as the same fura 2 loading and calibration methods were applied to both control and cardiomyopathic heart cells.

2.6.2. Determination of total Ca^{2+} level

After death, 220-day-old animals (8 CMH, 6 F1B) were autopsied; body and organs (heart, liver, lung) were weighed. Two methods were used for the histochemical demonstration of total Ca^{2+} levels: the Dahl and Mc-Gee-Russel alizarine red technique and the Von Kossa $AgNO_3$ technique (Martoja and Martoja, 1967). Briefly, tissue sections were embedded in paraffin and cut using conventional methods. Sections were exposed, in the first technique, to the following procedures: immersion for 2 min in 2% alizarine S, dehydration with acetone for 20 s and immersion in xylene. In the second technique, the procedures were: immersion (in obscurity) for 20 min in 2.5% silver nitrate, rinse in distilled water, immersion in 0.5% hydroquinone for 2 min, immersion for 2 min in 5% sodium thiosulphate and rinse in distilled water. Sections were then stained with Ramon y Cajal trichrome. Densitometry was used to determine the total Ca^{2+}, expressed in arbitrary absorbance units as mean ± S.E.M. We measured the total Ca^{2+} concentration in plasma (with the help of S. Philippakis), using the Calcium-MTB technique and an automatic UNI-KIT II apparatus (Roche Diagnostica, Switzerland). The following solutions were freshly prepared: solution A: 0.5 μM methylthymol blue, 55 μM hydroxy-8-quinoleinesulfonic acid, 0.625 μM ethanolamine, 23.75 μM sodium sulphite; solution B: 40.2 mM

EDTA (ethanol-diamine-tetraacetic acid, required to complex Mg). These solutions were unbuffered. We killed 3 F1Bs or 3 CMHs and immediately collected about 1 ml of blood from each heart; blood was pooled for each strain. The 3-ml pools were centrifuged at low speed for about 30 min and the plasma was collected. We introduced 5 μl of plasma into the apparatus with 30 μl of distilled water, 330 μl of solution A and finally 10 μl of solution B (starting solution). The absorbance was measured at 612 nm, 1 and 30 s after addition of solution B and the mean was calculated. The apparatus was calibrated before and after experimental measurements by replacing the 5 μl of plasma by 5 μl of 1, 2, 3, 4 mM of $CaCl_2$ dissolved in Krebs-Henseleit buffer.

2.7. Materials

Clostridium collagenase A (0.651 U/mg Lyo.) and laminin were purchased from Boehringer-Mannheim. Krebs-Henseleit bicarbonate buffer (K-3753), fura 2-AM, indo 1-AM, heparin and foetal bovine serum were purchased from Sigma. Fura 2-AM was prepared by solubilization in dimethyl sulphoxide containing pluronic F-127 acid (25% w/v). Trimetazidine was a gift from IRIS (Institut de Recherches Internationales Servier, France) and verapamil was purchased from Sigma. Serum trimetazidine and verapamil determinations were carried out by IRIS and the Centre Hospitalier Régional et Universitaire, Limoges, France, respectively.

2.8. Data analysis

All variables are presented as means ± standard errors of the mean (S.E.M.). The data were analysed by two-way analysis of variance (ANOVA; treatment and strain (F1B/CMH) as factors), followed, if significant, by the Newman-Keuls' test for pairwise comparisons (SigmaStat Software, Jandel Scientific). The number of animals in each group is indicated as *n*. Statistical significance was assumed at the 0.05 level.

3. Results

3.1. Survival study (n = 73)

The survival of 33 CMH, weighed weekly from birth to death, was followed. There were 3 deaths by 220 days (week 31), 9 deaths by 300 days (week 44), 19 by 380 days (week 55) and 32 deaths by 400 days (week 58). No death was observed in the F1B group (not shown) whereas more than 50% of the CMH animals had died by day 364 (Fig. 2). The longevity of CMHs (360 days) was about half that (700–900 days) of F1Bs. Of 10 CMH treated with verapamil, 7 animals died before 350 days and of 10 CMH treated with both verapamil and trimetazidine, 7 animals died before 350 days, with 2 at about 100 days (data not shown on Fig. 2) whereas only 1 of 20 animals on trimetazidine had died by 350 days. Survival was longer (560 days) in the group of trimetazidine-treated CMH ($n = 20$) than in untreated CMH (360 days) by about a 57% (Fig. 2).

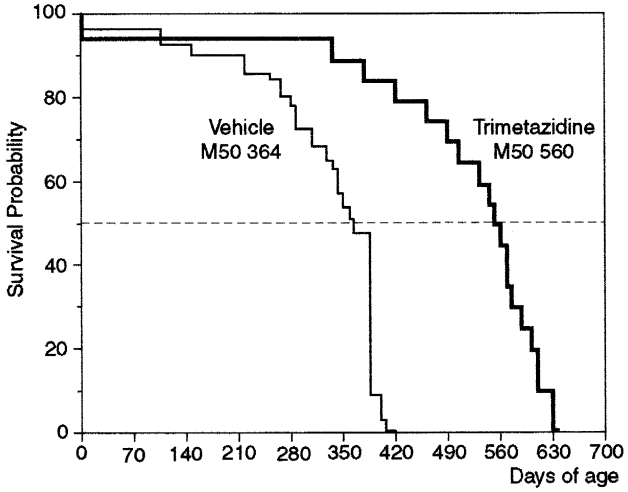

Fig. 2. Graph showing the survival rate of untreated BIO 14:6 cardiomyopathic hamsters (CMH; $n = 33$) and the effects of chronic trimetazidine administration (18 mg/kg per day) on the probability of survival (in %) of CMH ($n = 20$). Vehicle: distilled water. M50 indicates the age corresponding to the median probability of survival.

3.2. Anatomical features (n = 120)

Before 220 days, there was no difference between CMH and controls for body weight and organ weight to body weight ratio (Fig. 3). Cardiomyopathic hamsters had a lower body weight than F1B controls, at 220 days (−10%, $P < 0.05$) and 350 days (−14%, $P < 0.05$). Ventricular

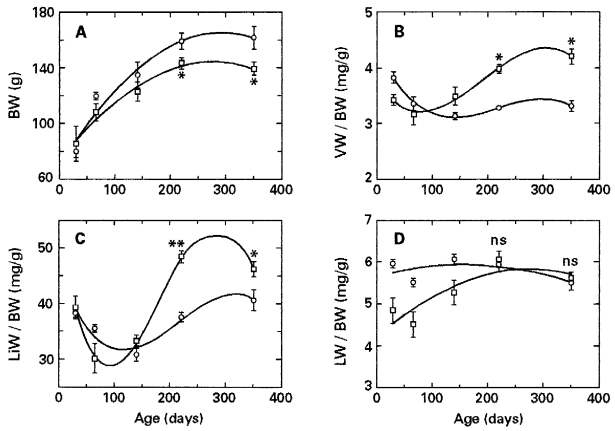

Fig. 3. Body weight, ventricle-, liver- and lung-weight to body weight ratio vs. age in cardiomyopathic hamsters (CMH, □) and controls (F1B, ○). (A) Body weight (BW; g) vs. age; (B) ventricular weight to body weight ratio (VW/BW; mg/g) vs. age; (C) liver weight to body weight ratio (LiW/BW; mg/g) vs. age; (D) lung weight to body weight ratio (LW/BW; mg/g) vs. age. * Significant differences between controls and CMH. * $P < 0.05$; * * $P < 0.001$; ns, not significant.

and liver hypertrophy was significant at 220 days (+22%, $P < 0.05$ and +29%, $P < 0.05$, respectively) and 350 days (+27%, $P < 0.05$ and +14%, $P < 0.05$, respectively). No lung hypertrophy was apparent either at 220 or 350 days (Table 1).

3.2.1. Comparison between CMH and treated CMH

ANOVA revealed a significant effect of treatment on body weight at 220 days ($F(1,30) = 5.47$, $P < 0.05$) but not at 350 days ($F(3,33) = 2.46$, ns), on ventricular hypertrophy at 220 days ($F(3,36) = 3.23$, $P < 0.05$) and 350 days ($F(3,35) = 4.48$, $P < 0.01$) and on liver hypertrophy at 220 days ($F(1,29) = 67.9$, $P < 0.0001$) and 350 days ($F(3,28) = 16.0$, $P < 0.0001$) (Table 1). Trimetazidine had a significantly greater effect on ventricular hypertrophy at 220 days (−12%, $P < 0.05$) than the other treatments, but had no effect on body weight. Although the body weight of the animals receiving verapamil and verapamil + trimetazidine was lower than that of animals receiving trimetazidine, the difference was not significant. The effect of trimetazidine seemed to be abolished by combination with verapamil and the value obtained was similar to the verapamil value. After 350 days, trimetazidine significantly reduced ventricular hypertrophy (−14%, $P < 0.05$) as did verapamil (−22%, $P < 0.05$) and the combination trimetazidine + verapamil (−15%, $P < 0.05$). No significant difference between treatments was observed. All treatments reduced liver hypertrophy at 220 days (trimetazidine: −28%, $P < 0.001$; verapamil: −25%, $P < 0.001$; trimetazidine + verapamil: −20%, $P < 0.001$) and at 350 days (trimetazidine: −29%, $P < 0.001$; verapamil: −18%, $P < 0.001$; trimetazidine + verapamil: −23%, $P < 0.001$) without there being significant difference between treatments (Table 1).

3.2.2. Comparison between treated CMH and treated F1B

ANOVA showed a statistically significant difference in body weight between groups (F1B/CMH) at 220 days ($F(1,63) = 25.7$; $P < 0.0001$) and at 350 days ($F(1,53) = 6.5$; $P < 0.05$) but revealed no significant differences between treatments, either at 220 days ($F(3,63) = 1.8$; ns) or at 350 days ($F(3,53) = 0.9$; ns). There was no differences between F1B and treated F1B at either ages (Table 1). The body weight of CMH treated with verapamil or the combination 'verapamil + trimetazidine' was significantly lower than that of treated F1B ($P < 0.05$) (Table 1).

There was a statistically significant difference in ventricle to body weight ratio between groups (F1B/CMH) at 220 days ($F(1,62) = 44.56$; $P < 0.0001$) but not at 350 days ($F(1,55) = 3.6$; ns); there was a significant difference between treatments, at 220 days ($F(3,62) = 3.8$; $P < 0.05$) but not at 350 days ($F(3,55) = 1.8$; ns). No difference was observed between F1B and treated F1B at either age (Table 1). Trimetazidine, at 220 days, reduced the ventricle to body weight ratio towards a value not different from that obtained in the treated F1B. At 350 days, all treatments reduced ventricle to body weight ratios towards values not different from those for the treated F1B group (Table 1).

There was no statistically significant difference in liver to body weight ratio between groups (F1B/CMH) at 220 days ($F(1,62) = 1.07$; ns) but there was a difference at 350 days ($F(1,48) = 4.5$; $P < 0.05$) and there was a significant difference between treatments, at 220 days ($F(3,62) = 7.9$; $P < 0.005$) and at 350 days ($F(3,48) = 6.4$; $P < 0.005$). The F1B and treated F1B groups were not different at the two ages (Table 1). After 220 days and 350 days, the ratios for CMH of all treatment groups were not significantly different from those for the treated F1B group (Table 1).

Table 1
Anatomical characteristics of the studied population

	Cardiomyopathic hamsters				Healthy hamsters			
	CMH	CMH-TMZ	CMH-V	CMH-TMZ + V	F1B	F1B-TMZ	F1B-V	F1B-TMZ + V
220 days								
Number of animals	17	5	9	7	14	4	4	4
BW	143.4 ± 3.8 [a]	145.4 ± 7.1	124.0 ± 4.4 [b,d]	124.8 ± 8.7 [b,d]	159.2 ± 5.8	162.6 ± 8.5	160.6 ± 8.5	155.7 ± 8.5
VW/BW	3.99 ± 0.08 [a]	3.52 ± 0.23 [b]	4.18 ± 0.16	4.13 ± 0.14	3.27 ± 0.04	3.08 ± 0.17	3.27 ± 0.17	3.50 ± 0.17
LW/BW	6.06 ± 0.20	5.67 ± 0.17	5.74 ± 0.25	5.96 ± 0.30	5.92 ± 0.13	5.46 ± 0.33	5.38 ± 0.33	5.56 ± 0.30
LiW/BW	48.5 ± 1.0 [a]	34.9 ± 2.1 [c]	36.4 ± 2.5 [c]	38.8 ± 1.2 [c]	37.5 ± 0.8	37.4 ± 2.1	40.9 ± 2.2	37.6 ± 2.2
350 days								
Number of animals	23	5	4	4	8	4	4	4
BW	139.3 ± 4.4 [a]	162.4 ± 4.7	143.2 ± 4.7	146.0 ± 2.7	162 ± 8	161.6 ± 8.4	160.4 ± 8.1	161.8 ± 8.4
VW/BW	4.21 ± 0.14 [a]	3.62 ± 0.11 [b]	3.26 ± 0.10 [b]	3.56 ± 0.10 [b]	3.31 ± 0.17	3.37 ± 0.24	3.44 ± 0.24	3.38 ± 0.20
LW/BW	5.62 ± 0.10	5.21 ± 0.20	4.71 ± 0.10	4.44 ± 0.20	5.48 ± 0.15	5.46 ± 0.20	5.38 ± 0.21	5.51 ± 0.21
LiW/BW	46.3 ± 1.3 [a]	33.0 ± 1.5 [c]	38.0 ± 1.2 [c]	35.7 ± 1.5 [c]	40.7 ± 1.5	40.1 ± 2.1	41.9 ± 2.1	41.9 ± 2.2

F1B controls (healthy); CMH, untreated cardiomyopathic hamsters; CMH-TMZ/F1B-TMZ, CMH/F1B treated with trimetazidine (18 mg/kg); CMH-V/F1B-V, CMH/F1B treated with verapamil (120 mg/kg); CMH-TMZ + V/F1B-TMZ + V, CMH/F1B treated with a combination of trimetazidine and verapamil (same doses). VW, ventricular weight; LW, lung weight; LiW, liver weight; BW, body weight. Values are means ± S.E.M. Only statistically significant differences are shown. [a] $P < 0.05$ vs. F1B; [b] $P < 0.05$ and [c] $P < 0.001$ vs. CMH; [d] $P < 0.05$ vs. treated F1B.

3.3. Intracellular Ca^{2+} levels ($n = 90$)

3.3.1. Cell morphology

Only rod-shaped cells, well attached to slides, with clear cross-striations were used for Ca^{2+} studies by laser scanning cytometry. The morphology of single cardiac myocytes was also assessed by polarization microscopy. Myocytes from cardiomyopathic hamsters were slightly but significantly wider (measured at the middle of the long axis) and longer (maximum length) than control myocytes (Fig. 4). Cardiomyopathic hamster myocytes had more ends that appeared irregular than did the control myocytes and displayed more digitation than did the normal myocytes. Morphological data were obtained by laser scanning cytometry from 4 F1B and 4 CMH, and about 10 cells from each heart were analysed (Table 2). The shape factor, determined by the Meridian software, is 1 for a sphere and increases with the asymmetry of the cell.

Table 2
Dimensions of isolated ventricular myocytes

Group	Length (μm)	Width (μm)	Shape factor	Length/width
CMH	91.4 ± 1.6	14.2 ± 0.7	2.3 ± 0.2	6.4 ± 0.1
F1B	70.6 ± 1.9	11.4 ± 0.6	1.8 ± 0.1	6.1 ± 0.1
P [a]	< 0.001	< 0.05	< 0.05	< 0.05

Values are means ± S.E.M., $n \cong 40$ myocytes from 4 hearts. CMH, BIO 14:6 cardiomyopathic hamsters (7 months old); F1B, normal hamsters.
[a] Unpaired, two-tailed t-test.

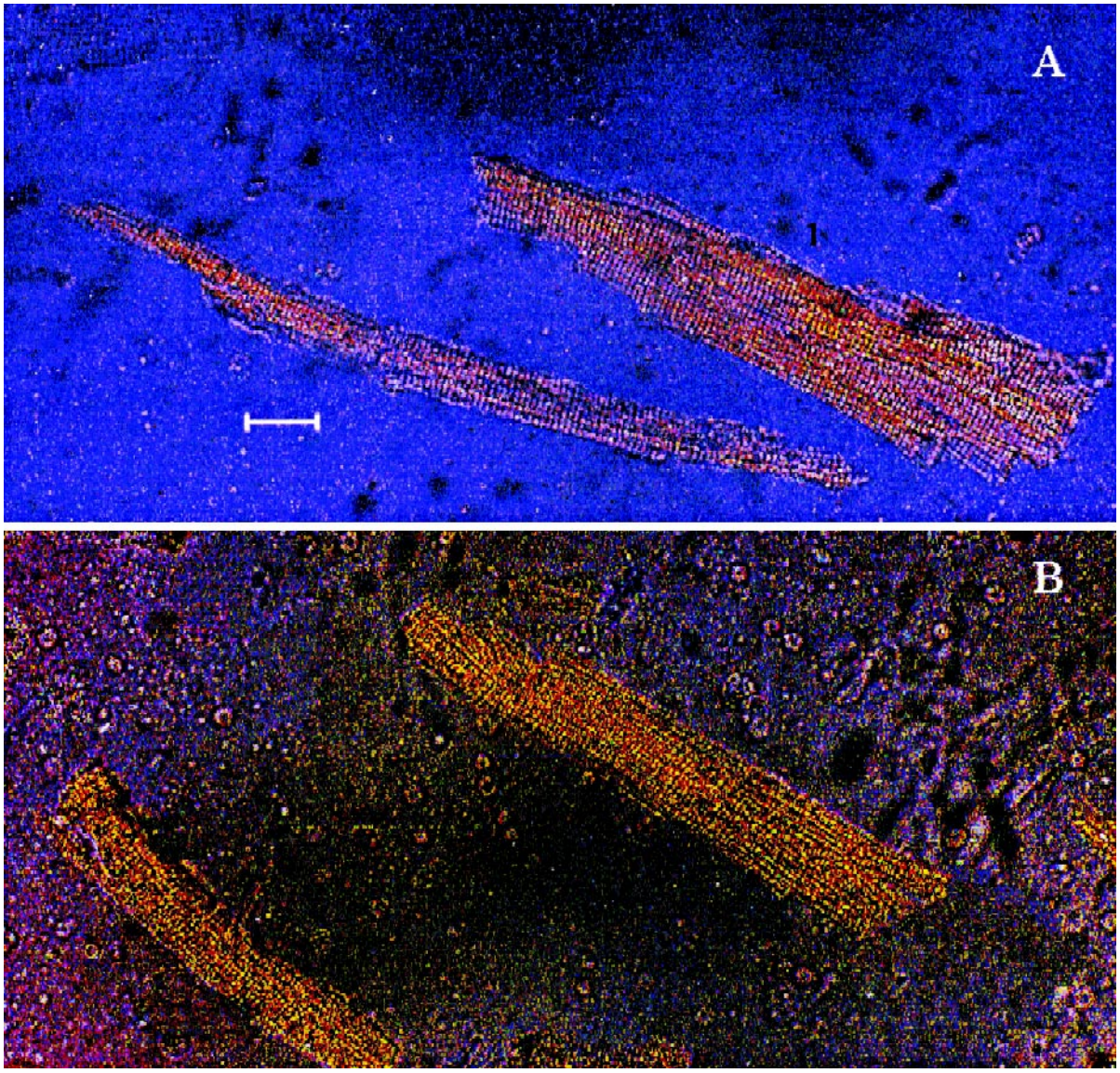

Fig. 4. Cells isolated from a 7-month-old BIO 14:6 cardiomyopathic hamster (A) (90% of type-1 cardiac cells were observed consistently in all preparations) and control hamster (B). Bar = 10 μm. Morphology was assessed by polarization microscopy.

3.3.2. Total Ca^{2+} ($n = 52$)

Fifty-two animals were processed for this study. For each animal, the mean value for 5 slides each containing about 10–15 sections was determined. There were no significant differences between right and left ventricles (data not shown). Both methods gave the same qualitative finding: there was an accumulation of total Ca^{2+} in the BIO 14:6 groups, with no difference between 220 and 350 days (data not shown). The accumulation factor was 1.3 ± 0.1 ($P < 0.001$; $n = 8$ CMH/$n = 6$ F1B) with alizarine red and 1.9 ± 0.4 ($P < 0.001$; $n = 8$ CMH/$n = 6$ F1B) with silver nitrate. In treated CMHs ($n = 24$) the total Ca^{2+} level was similar to that in F1Bs (Fig. 5). Total Ca^{2+}, determined using methylthymol blue, was 3 ± 0.2 mM and 2.7 ± 0.2 mM in extracellular fluids, in CMH and F1B, respectively.

3.3.3. Cytosolic Ca^{2+} ($n = 30$)

Cytosolic Ca^{2+} at rest was determined in living cells without electrical stimulation, at an external Ca^{2+} concentration of 0.6 mM (see Section 2). Each reported value is the average of 3 cellular suspensions each containing about 10^6 cells, of which about 80% were rod shaped. The mean Ca^{2+} in cardiomyopathic myocytes was 543 ± 28 nM, about 4-fold higher than that (123 ± 17 nM) in normal cells ($P < 0.001$) (Fig. 6). No significant differences were found in the R_{max} ratio (4.82 ± 0.47 vs. 4.62 ± 0.38) or R_{min} ratio (0.92 ± 0.03 vs. 0.85 ± 0.03) between the cardiomyopathic ($n = 5$) and F1B ($n = 8$) animals. These results suggest that the properties of the intracellular fluorescent probe, fura 2, are similar in these 2 different groups. This should therefore allow valid comparative fluorometric analysis. The Ca^{2+} overaccumulation determined by spectrofluorometry was checked by laser scanning analysis, which revealed differences in Ca^{2+} levels between normal and cardiomyopathic cells. The ratios of the total fluorescence were 2.5 ± 0.1 in CMH and 1.5 ± 0.1 in F1B ($P < 0.05$), giving a factor of 1.7 ± 0.2 between the two (Fig. 7).

The cytosolic Ca^{2+} concentration was reduced by 54% ($P < 0.001$) in the trimetazidine group, by 39% ($P < 0.005$) in the verapamil group and by 48% ($P < 0.01$) in the trimetazidine + verapamil group (Fig. 6). There were no significant differences between groups.

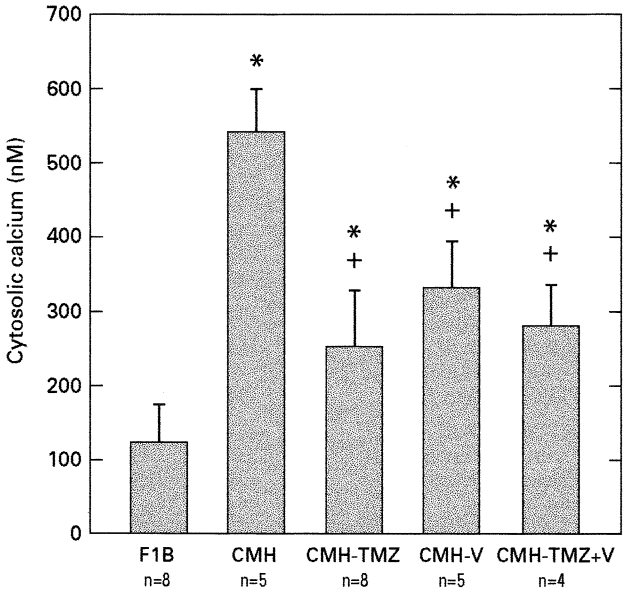

Fig. 6. Cytosolic Ca^{2+} concentrations in the heart of 220-day-old controls (F1B), cardiomyopathic Syrian hamsters (CMH) and CMH treated with trimetazidine (CMH-TMZ), verapamil (CMH-V) or with a combination of both (CMH-TMZ + V) from age 30 to 220 days. Cytosolic Ca^{2+} concentrations (at 0.6 mM external Ca^{2+}) were assayed by spectrofluorometry using fura 2. The data are expressed in nM as means ± S.E.M. * Statistically significantly different from the F1B group, * $0.001 < P < 0.005$. + Statistically significantly different from the CMH group, + $0.001 < P < 0.005$. The values for the 3 treatment groups were not significantly different.

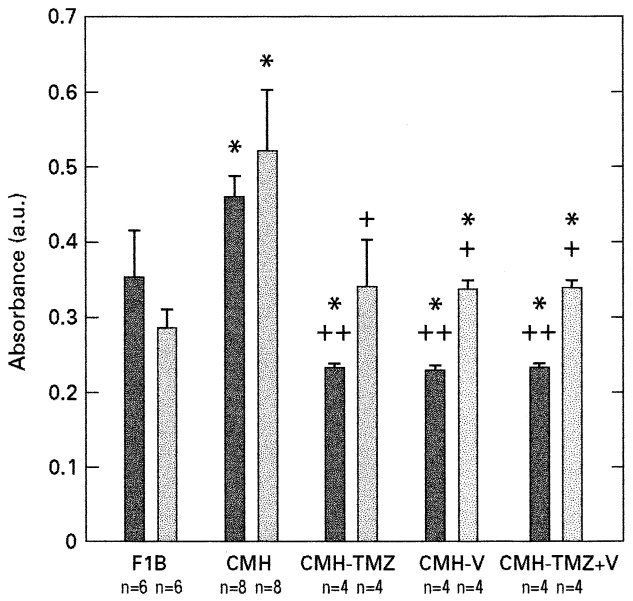

Fig. 5. Relative amounts of total Ca^{2+} in the heart of 220-day-old controls (F1B), cardiomyopathic Syrian hamsters (CMH) and CMH treated with trimetazidine (CMH-TMZ), verapamil (CMH-V) or with a combination of both (CMH-TMZ + V) from age 30 to 220 days. The Ca^{2+} levels were assayed by histochemical techniques, using alizarine red (black bars) or silver nitrate (grey bars), and determined by densitometric analysis. The data are expressed in arbitrary units (a.u.) as means ± S.E.M. * Statistically significantly different from the F1B group, * $0.001 < P < 0.02$. + Statistically significantly different from the CMH group, ++ $P < 0.001$ and + $0.005 < P < 0.01$. The values for the 3 treatment groups were not significantly different.

3.4. Plasma concentrations of trimetazidine and verapamil

Plasma levels were constant after 8 days, 18 days and 32 days of trimetazidine treatment and after 30 days of verapamil treatment. The plasma concentration of trimetazidine was 16.9 ± 1.4 ng/ml (about 75 nM; $n = 9$ CMH). The plasma concentration of verapamil was 29.6 ± 6.9 ng/ml (about 60 nM; $n = 4$ CMH). *nor*-Verapamil,

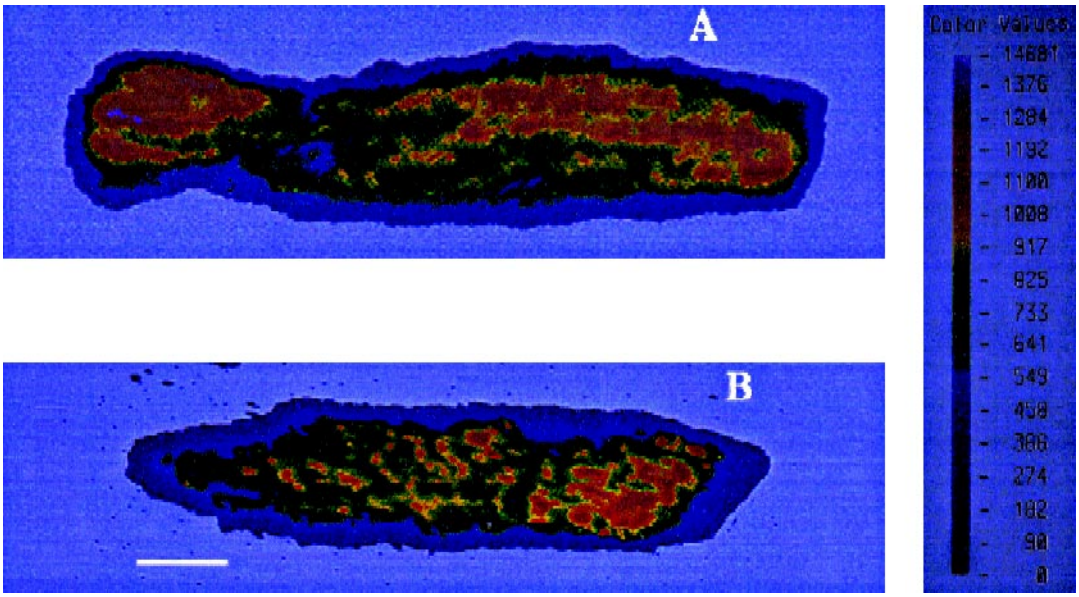

Fig. 7. Fluorescence localization and measurement (arbitrary units) in intracellular Ca^{2+} on adherent cardiac cells from a cardiomyopathic hamster (CMH) (A) and normal hamster (F1B) (B). Analysis was performed by laser scanning cytometry (Institut Pasteur, Paris) using the indo 1 marker. Bar = 10 μm. These cells were chosen as the best representative samples for Ca^{2+} level distribution.

the major active metabolite of verapamil, which may be responsible for a small proportion of the overall pharmacological effect, was also assayed. Its concentration was 15.2 ± 3.8 ng/ml (about 30 nM; $n = 4$ CMH).

4. Discussion

We have shown that long-term trimetazidine therapy applied to CMHs, an animal model of cardiomyopathy, leads to a significant decrease in the signs of the disease: reduction in the heart and liver hypertrophy, full disappearance of the total Ca^{2+} overload, noticeable decrease in the abnormally high cytosolic Ca^{2+} concentration in cardiomyopathic myocardial cells and improvement of survival of CMH.

The estimated level of resting intracellular Ca^{2+} was comparable to those previously reported for 240-day-old BIO 14:6 hamsters by Sen et al. (1990) using the single cell technique (121 ± 28 nM) and for adult rat myocytes measured with either fura 2 (90 nM, 155 nM, 100 nM) or indo 1 (136 nM) (cited in Gomez et al., 1994). We used a concentration of extracellular Ca^{2+} of 0.6 mM because it has been shown (Sen et al., 1990) that (i) cardiomyopathic myocytes can tolerate an extracellular Ca^{2+} concentration of 0.6 mM in Krebs-Henseleit medium with only about 15% of cells rounding up and (ii) at such a low Ca^{2+} concentration, the difference between Ca^{2+} in CMH myocytes and Ca^{2+} in normal myocytes is large. At higher extracellular Ca^{2+} concentrations (1.5 mM and 2 mM), the difference is less substantial (Sen et al., 1990). Moreover, although cells could tolerate 1 mM Ca^{2+} in our study, the measurements of cytosolic Ca^{2+} at an external Ca^{2+} concentration of 2 mM did not give good results because of the high and limiting percentage of round cells (about 40%). Thus, 0.6 mM was chosen although it is lower than the physiological concentration. Indeed, total Ca^{2+} is about 3 mM in extracellular fluids (see Section 3) but about 2/3 of this is Ca^{2+} bound to proteins, phosphate anions, etc. Thus, physiological free Ca^{2+} values are normally 0.9–1 mM. The total Ca^{2+} overload factor, determined as absorbance ratios using silver nitrate (1.9 ± 0.4) and alizarine red (1.30 ± 0.1), probably mainly reflects the sarcoplasmic reticulum Ca^{2+} level (Katz, 1992). A 2-fold elevation of Ca^{2+} in a population of mitochondria isolated from 21- to 412-day-old cardiomyopathic hamster hearts has been observed (Wrogemann and Nylen, 1978). According to the authors, this population may come from areas of the heart that are just undergoing cell necrosis. The cytosolic Ca^{2+} overload in myocytes isolated from CMH is not well documented. Sen et al. (1990) measured an overload factor of 2 in stimulated and unstimulated myopathic cells. The difference between our results (we found a 4-fold increase) and his could be due to the experimental preparation (single cell vs. perfused heart) or the strains studied. Analysis by laser scanning cytometry led us to corroborate our results by a qualitative and complementary approach addressing the cell Ca^{2+} in different ways. Nevertheless, the accumulation factor (of about 1.7) between normal and cardiomyopathic cells was smaller than that determined with cell suspensions. This difference could be due to the properties of the fluorescent dye (indo 1 vs. fura 2) or to the experimental preparation (single cell vs. cell suspension). Cardiocytes from cardiomyopathic hamsters were also longer and wider than those from normal animals. Although we did not determine cell volume, this suggests

cellular hypertrophy, in agreement with previous morphological measurements by others (Sorenson et al., 1985; Sen et al., 1990; Gilloteaux et al., 1990). We found our cells not to be as long and wide as the cells described in these studies. The difference could be due to the different strains studied, the method of cell examination (under a coverslip vs. in a well) or the matrix used (laminin).

This localized Ca^{2+} overload has been suggested to be the consequence of spasms of the microcirculation (Sen et al., 1990), which, producing transient focal ischaemia, could be a cause of cardiomyopathy (Natelson et al., 1991; Conway et al., 1994). The genetically altered cardiomyopathic heart includes several of the pathologic components of ischaemic injury (Jasmin and Proschek, 1984): dysfunction of energy production (ATP depletion) (Tian et al., 1996), acidosis and overproduction of free fatty acids and oxygen-derived free radicals (Fukuchi et al., 1991) responsible for disturbed cellular homeostasis and, consequently, for the rise in cellular Ca^{2+} (Reiter et al., 1991; Perennec et al., 1992). This tends to block many vital enzymatic functions and leads to necrosis (Gilloteaux et al., 1990). Hypertrophy is a compensatory adaptative process to the cell loss which occurs following myocardial necrosis (Momomura et al., 1993). Thus, it is valuable to use a specific drug therapy to limit cell injury, at least in part, through the preservation of normal Ca^{2+} homeostasis. Trimetazidine is appropriate due to its anti-ischaemic properties and its lack of haemodynamic effects (Detry et al., 1994).

The effects of trimetazidine on Ca^{2+} are comparable to those obtained with verapamil, administered at therapeutic doses and under the same conditions: reduction of cytosolic and total Ca^{2+} levels. Moreover, trimetazidine had a positive and specific effect, abolishing CMH ventricular hypertrophy. This effect was detected after 220 and 350 days. That this effect is due to an action on the Ca^{2+} level is unlikely because no effect on hypertrophy could be demonstrated at 220 days with verapamil, a well-known inhibitor of L-type Ca^{2+} channel (Finkel, 1993). This suggests that the mechanism of the hypertrophy-reducing effect of trimetazidine may be different from that of verapamil and that possibly neither depend on altering the abnormal Ca^{2+} level.

The mechanism(s) underlying the beneficial effect of trimetazidine are still unknown (Fantini et al., 1994). Prevention of cell damage and consequently myocyte loss through an anti-oxidant effect (Maupoil et al., 1990) could explain the reduction of ventricular hypertrophy achieved with trimetazidine. Another possibility is that trimetazidine, by limiting acidosis (Renaud, 1988) and by increasing intrinsic cardiac H^+ buffering power (β_i) (Lagadic-Gossmann et al., 1996), slows Na^+/H^+ exchange. Consequently, trimetazidine would reduce Na^+ influx and thus Ca^{2+} influx via Na^+/Ca^{2+} exchange (Verdonck et al., 1993). Since an increase in cellular Na^+ content may be the driving force for cellular swelling during ischaemia (Askenasy and Navon, 1996), trimetazidine, by limiting Na^+ influx, may prevent the volume modification that causes hypertrophy. Thus, by preventing the Na^+-linked Ca^{2+} overload, trimetazidine would limit tissue necrosis and ventricular hypertrophy. Possibly both phenomena may be involved in hypertrophy because the oxygen radical-mediated myocardial damage may have important functional consequences on membrane exchanges. Nevertheless, these effects are only observed at concentrations higher than those we studied. Thus, we cannot exclude possible cardiac depression as a result of these doses. Further investigations, including contractile studies of hearts, are needed to clarify the possible direct cardiovascular effects of our doses.

The effect of verapamil on ventricular hypertrophy was 'visible' after 350 days but not 220 days. Verapamil may thus act by a long-duration mechanism, different from a direct anti-Ca^{2+} effect, possibly through its peripheral vasodilator action (Godfraind et al., 1991; Raizada et al., 1994). This agrees with the fact that verapamil modulates the CMH myosin phenotype (D'hahan et al., unpublished data) in favour of the V_1 form, shown to be in inverse ratio to the degree of ventricular hypertrophy (Mercadier et al., 1981). Thus, trimetazidine, although sharing the same anti-Ca^{2+} properties, seems more efficient than verapamil in preventing hypertrophy, since it acts earlier in the disease process and also prolongs survival. Clinical studies have shown positive effects of combining trimetazidine with a Ca^{2+} antagonist such as nifedipine (Brochier et al., 1986) or a β-adrenoceptor antagonist (Michaelides et al., 1987), but as far as we know, the combination trimetazidine + verapamil has never been studied. In our study, the detectable effect of trimetazidine on ventricular hypertrophy after 220 days was abolished when the drug was given in combination with verapamil. This suggests an interaction in favour of verapamil, which may prevent the action of trimetazidine and reduce CMH survival. Nevertheless, at 350 days, the CMH-trimetazidine + verapamil effect upon hypertrophy was just as strong as that of CMH-trimetazidine or CMH-verapamil. It is possible that this is the maximum effect possible and that the two effects are simply not additive. Further investigations are needed to clarify the characteristics of this combination.

A major question concerns the therapeutic relevance of the effects reported here. We used trimetazidine concentrations that correspond to the therapeutic range, i.e., to a trimetazidine concentration found in vivo and in vitro to limit the consequences of ischaemia (in the range 0.1–1 μM) (Harpey et al., 1989). The plasma concentration of verapamil was about 60 nM, which also corresponds to the therapeutic range (Freedman et al., 1981).

One of the original findings of our study is that trimetazidine, administered as a long-term monotherapeutic intervention, had the same beneficial effects as a conventional treatment (verapamil) in preventing a high myocardial Ca^{2+} content, but more efficiently reduced ven-

tricular hypertrophy and improved the survival of CMH. This study also demonstrates the usefulness of the model for evaluating compounds with anti-ischaemic properties. Finally, the safety of trimetazidine, assessed in clinical trials, and its widespread use, especially in Japan and France, are important considerations in favour of this agent as a candidate for preventing human congestive heart failure of similar aetiology.

Acknowledgements

A preliminary account of this work was presented at the XXIV European Muscle Conference (European Society for Muscle Research), Florence, Italy, September 13–16, 1995. Part of this work was supported by grants from the Institut de Recherches Internationales Servier (IRIS, France) and by predoctoral fellowships of Institut de Formation Supérieure Bio Médicale (IFSBM, Villejuif, France) and IRIS to Nathalie D'hahan. We thank Dr. Patrick Hannaert from INSERM U400, Faculté de Médecine (Créteil, France) and Dr. Renée Ventura-Clapier from INSERM U446, Faculté de Pharmacie (Châtenay-Malabry, France) for helpful discussions.

References

Askenasy, N., Navon, G., 1996. Volume-related activities of sodium ion transporters: multinuclear NMR studies of isolated rat hearts. Am. J. Physiol. 271, H94–H106.

Boddeke, E., Hugtenburg, J., Jap, W., Heynis, J., Van Zwieten, P., 1989. New anti-ischaemic drugs: cytoprotective action with no primary haemodynamic effects. Trends Pharmacol. Sci. 10, 397–400.

Brochier, M., Demange, J., Ducloux, G., Monpère, C., Warin, J.F., 1986. Therapeutic value of a combination of trimetazidine and a Ca^{2+} antagonist for the treatment of chronic artery disease. Controlled, double-blind study against placebo. Presse Med. 15, 1783–1787.

Brottier, L., Barat, J.L., Combe, C., Boussens, B., Bonnet, J., Bricaud, H., 1990. Therapeutic value of a cardioprotective agent in patients with severe ischaemic cardiomyopathy. Eur. Heart J. 11, 207–212.

Chiercha, S.L., Fragasso, G., 1993. Metabolic management of ischaemic heart disease. Eur. Heart J. 14 (Suppl. G), 2–5.

Conway, R.S., Natelson, B.H., Chen, W.H., Ting, W., 1994. Enhanced coronary vasoconstriction in the Syrian myopathic hamster supports the microvascular spasm hypothesis. Cardiovasc. Res. 28, 320–324.

Dalla-Volta, S., Maraglino, G., Della-Valentino, P., Desideri, A., 1990. Comparison of trimetazidine with nifedipine in effort angina: a double-blind cross-over study. Cardiovasc. Drugs Ther. 4, 853–860.

Davidoff, A.J., Gwathmey, J.K., 1994. Pathophysiology of cardiomyopathiesPart I. Animal models and humans. Curr. Opin. Cardiol. 9, 357–368.

Detry, J.M., Sellier, P., Pennaforte, S., Cokkinos, D., Dargie, H., Mathes, P., 1994. Trimetazidine: a new concept in the treatment of angina. Comparison with propranolol in patients with stable angina. Br. J. Clin. Pharmacol. 37, 279–288.

Devynck, M.A., Le Quan Sang, K.H., Joulin, Y., Mazeaud, M., 1993. Acute membrane effects of trimetazidine in human platelets. Eur. J. Pharmacol. 245, 105–110.

Factor, S.M., Cho, S., Scheuer, J., Sonnenblick, E.H., Malhotra, A., 1988. Prevention of hereditary cardiomyopathy in the Syrian hamster with chronic verapamil therapy. J. Am. Cell. Cardiol. 12, 1599–1604.

Fantini, E., Demaison, L., Sentex, E., Grynberg, A., Athias, P., 1994. Some biochemical aspects of the protective effect of trimetazidine on rat cardiomyocytes during hypoxia and reoxygenation. J. Mol. Cell. Cardiol. 26, 949–958.

Finkel, M.S., 1993. Verapamil regulation of a defective SR release channel in the cardiomyopathic hamster. Life Sci. 52, 1109–1119.

Freedman, S.B., Richmond, D.R., Ashley, J.J., Kelly, D.T., 1981. Verapamil kinetics in normal subjects and patients with coronary artery spasm. Clin. Pharmacol. Ther. 30, 644–652.

Fukuchi, T., Kobayashi, A., Kaneko, M., Ichiyama, A., Yamazaki, N., 1991. Possible involvement of free radicals and antioxidants in the early stages of the development of cardiomyopathy in BIO 14.6 Syrian hamster. Jpn. Heart J. 32, 655–666.

Gilloteaux, J., Bissler, J.J., Kondolios, P., Jarjoura, D., 1990. Cardiomyocyte aging and hypertrophy: atrial and ventricular changes in normal and myopathic Syrian hamsters. J. Sub. Cytol. Pathol. 22, 249–257.

Godfraind, T., Kazda, S., Wibo, M., 1991. Effects of a chronic treatment by nisoldipine, a calcium antagonistic dihydropyridine, on arteries of spontaneously hypertensive rats. Circ. Res. 68, 674–682.

Gomez, J.-P., Potreau, D., Raymond, G., 1994. Intracellular Ca^{2+} transients from newborn rat cardiomyocytes in primary culture. Cell Calcium 15, 265–275.

Grynkiewicz, G., Poenie, M., Tsien, R.Y., 1985. A new generation of Ca^{2+} indicators with greatly improved fluorescence properties. J. Biol. Chem. 260, 3440–3450.

Hanton, G., Barnes, P., Shepperson, N.B., Walley, R., 1993. Effects of hydrochlorothiazide and captopril on the survival and heart weight of cardiomyopathic hamsters. Res. Commun. Chem. Pathol. Pharmacol. 81, 159–166.

Harpey, C., Clauser, P., Labrid, C., Freyria, J.L., Poirier, J.P., 1989. Trimetazidine, a cellular anti-ischemic agent. Cardiovasc. Drug Rev. 6, 292–312.

Jasmin, G., Proschek, L., 1984. Calcium and myopathic cell injury. An appraisal in the cardiomyopathic hamster. Can. J. Physiol. Pharmacol. 62, 891–898.

Kagiya, T., Hori, M., Iwakura, K., Iwai, K., Watanabe, Y., Uchida, S., Yoshida, H., Kitabatake, A., Inoue, M., Kamada, T., 1991. Role of increased α_1-adrenergic activity in cardiomyopathic Syrian hamster. Am. J. Physiol. 260, H80–H88.

Katz, A.M., 1992. Physiology of the Heart, 2nd ed. Raven Press, New York, NY, p. 23.

Lagadic-Gossmann, D., Le Prigent, K., Feuvray, D., 1996. Effects of trimetazidine on pHi regulation in the rat isolated ventricular myocyte. Br. J. Pharmacol. 117, 831–838.

Lavanchy, N., Martin, J., Rossi, A., 1987. Anti-ischaemic effects of trimetazidine: ^{31}P-NMR spectroscopy in the isolated rat heart. Arch. Int. Pharmacodyn. 286, 97–110.

Martoja, R., Martoja, A., 1967. Initiation aux Techniques de l'Histologie Animale. Masson, Paris, pp. 233–237.

Maupoil, V., Rochette, L., Tabard, A., Clauser, P., Harpey, C., 1990. Direct measurement of free radical generation in isolated rat heart by electron paramagnetic resonance spectroscopy: effect of trimetazidine. In: Emerit (Ed.), Antioxidants in Therapy and Preventive Medecine. pp. 373–376.

Mercadier, J.-J., Lompre, A.-M., Wisnewsky, C., Samuel, J.-L., Bercovicci, J., Swynghedauw, B., Schwartz, K., 1981. Myosin isoenzymic changes in several models of rat cardiac hypertrophy. Circ. Res. 49, 525–532.

Métézeau, P., Kieffer, H., Lamy, G., Delamare, G., 1993. Laser scanning cytometry for analysis and preparation [in French]. Pathol. Biol. 41, 276–280.

Michaelides, A.P., Vysoulis, G.P., Bonoris, P.E., Psaros, Th.K., Papadopoulos, P.D., Toutouzas, P.K., 1987. Beneficial effects of trimetazidine in patients with stable angina under beta-blockers. Cardiovasc. Drug Ther. 1, 268–274.

Momomura, S.-I., Nagai, Y., Ogawa, T., Bessho, M., Yamashita, H., Serizawa, T., 1993. Increased tolerance of ventricular function and

energy metabolism to hypoxia in cardiomyopathic hamsters. J. Mol. Cell. Cardiol. 25, 551–562.

Natelson, B.H., Tapp, W.N., Drastal, S., Suarez, R., Ottenweller, J.E., 1991. Hamsters with coronary vasospasm are at increased risk from stress. Psychol. Med. 53, 322–331.

Perennec, J., Pocholle, W.P., Hatt, P.Y., Crozatier, B., 1992. Cardiac ultrastructure abnormalities in Syrian hamsters with spontaneous cardiomyopathy or subjected to cardiac overloads. Basic Res. Cardiol. 87, 54–64.

Pocock, J.M., Nicholls, D.G., 1992. A toxin (Aga-GI) from the venom of the spider *Agelenopsis aperta* inhibits the mammalian presynaptic Ca^{2+} channel coupled to glutamate exocytosis. Eur. J. Pharmacol. 226, 343–350.

Raizada, V., Pathak, D., Nakouzi, A., Malhotra, A., 1994. Prevention of age-related V_1 myosin isozyme decrement in the adult rat heart. J. Mol. Cell. Cardiol. 26, 293–296.

Reiter, R.J., White, T., Lerchl, A., Stokkan, K.A., Rodriguez, C., 1991. Attenuated nocturnal rise in pineal and serum melatonin in a genetically cardiomyopathic Syrian hamster with a deficient calcium pump. J. Pineal Res. 11 (3-4), 156–162.

Renaud, J.F., 1988. Internal pH, Na^+ and Ca^{2+} regulation by trimetazidine during cardiac cell acidosis. Cardiovasc. Drugs Ther. 1, 677–686.

Sen, L., O'Neill, M., Marsh, J.D., Smith, T.W., 1990. Myocyte structure, function and Ca^{2+} kinetics in the cardiomyopathic hamster heart. Am. J. Physiol. 259, H1533–H1543.

Sonnenblick, E.H., Fein, F., Capasso, J.M., Factor, S.M., 1985. Microvascular spasm as a cause of cardiomyopathy and the calcium-blocking agent verapamil as potential primary therapy. Am. J. Cardiol. 55, 179B–184B.

Sorenson, A.L., Tepper, D., Sonnenblick, E.H., Robinson, T.F., Capasso, J.M., 1985. Size and shape of enzymatically isolated ventricular myocytes from rats and cardiomyopathic hamsters. Cardiovasc. Res. 19, 793–799.

Tian, R., Nascimben, L., Kaddurah-Daouk, R., Ingwall, J.S., 1996. Depletion of energy reserve via the creatine kinase reaction during the evolution of heart failure in cardiomyopathic hamsters. J. Mol. Cell. Cardiol. 28, 755–765.

Van Zwieten, P.A., 1985. Drug Targets in Unstable Angina: Current Concepts and Management. Schattauer Verlag, pp. 151–157.

Venkatakrishnan, R., Rourke, A.W., 1979. The structure, function and turnover of cardiac myosin in normal and myopathic Syrian hamsters. Lab. Invest. 41, 198–205.

Verdonck, L., Borgers, M., Verdonck, F., 1993. Inhibition of sodium and calcium overload pathology in the myocardium: a new cytoprotective principle. Cardiovasc. Res. 27, 349–357.

Voisin, E.M., Ruthsatz, M., Collins, J.M., Hoyle, P.C., 1990. Extrapolation of animal toxicity to humans: interspecies comparisons in drug development. Regul. Toxicol. Pharmacol. 12, 107–116.

Wrogemann, K., Nylen, E.G., 1978. Mitochondrial calcium overloading in cardiomyopathic hamsters. J. Mol. Cell. Cardiol. 10, 185–195.